Aerosol and Air Quality Research, 12: 615–628, 2012

ISSN: 1680-8584 print / 2071-1409 online
doi: 10.4209/aaqr.2011.11.0191

Air Quality Modeling for a Strong Dust Event in East Asia in March 2010

Xiao Han[1], Cui Ge[2], Jinhua Tao[3], Meigen Zhang[1*], Renjian Zhang[4]

[1] *State Key Laboratory of Atmospheric Boundary Layer Physics and Atmospheric Chemistry, Institute of Atmospheric Physics, Chinese Academy of Sciences, Beijing 100029, China*
[2] *Department of Earth and Atmospheric Sciences, University of Nebraska – Lincoln, NE, USA*
[3] *State Key Laboratory of Remote Sensing Science, Jointly Sponsored by Institute of Remote Sensing Applications of Chinese Academy of Sciences and Beijing Normal University, Beijing 100101, China*
[4] *Key Laboratory of Regional Climate-Environment for East Asia, Institute of Atmospheric Physics, Chinese Academy of Sciences, Beijing 100029, China*

ABSTRACT

In 19 and 20 March 2010, the annual strongest dust event occurred over East Asia, for the reports from National Meteorological Center of CMA (China Meteorological Administration) showed that 16 provinces (cities) of China were affected by the dust storm, and the air pollution index (API) given by Ministry of Environment Protection of China exceeded 300 in 13 Chinese cities. An air quality modeling system RAMS-CMAQ was employed to simulate the spatial and temporal features of this dust event, and analyze its impacts on air quality and regional radiative effect in East Asia. The modeled mass concentrations and aerosol optical depth (AOD) of dust and other aerosol species are generally in good agreement with surface observations and satellite measurements. Numerical analysis shows that the dust storm generated over Mongolia and west of Inner Mongolia, and swept central, eastern and southern China, also including the East China Sea. The highest value of dust concentration exceeded 3000 μg/m^3 in the source area and waved from 200 to 1000 μg/m^3 in the downstream areas. The high AOD values mainly contributed by dust ranged from 0.5 to 1.5, which means the regional visibility and radiation would be significantly impacted by the dust particles. The direct radiative forcing of dust was also obviously strong with values from –5 to –30 W/m^2 appeared over the regions where dust storm swept. This value is almost equal to the radiative effect of total aerosol components over these areas.

Keywords: CMAQ; Asian dust event; AOD; Radiative forcing.

INTRODUCTION

Dust storms occurred in East Asia is one of the severely disastrous weather that may have a long-term, harmful effect and may destroy the atmospheric and ecological environment in the arid and semiarid regions. The long-range transport of dust could reach south of China, Taiwan, Korea, southeast Asia (Satheesh and Ramanathan, 2000; Chun *et al*., 2002; Kurosaki and Mikami, 2003; Chen *et al*., 2004), and even North America (Tratt *et al*., 2001; Sassen, 2002). By changing the radiative flux, the dust particle also has climate effect. IPCC (2007) reported that the global average value of dust direct radiative forcing is ranging from –0.6 to 0.4 W/m^2, and the uncertainties are still large. Previous studies show that the dust storm over East Asia could significantly impact the local atmospheric optical properties and radiative forcing (Qian *et al*., 2002; Zhang *et al*., 2003b; Wang *et al*., 2004), and then influence the region climate.

In the last decade, numerous research works have focused on the Asian dust storm by monitoring and modeling. Zhang *et al*. (2003a) presented the daily aerosol observed results from six sites in China, and the burden of PM_{10} at four Chinese cities during spring 2001 for improving the understanding of chemical and physical properties of dust aerosol. The size distribution of elemental components of particles in several dust events in Beijing were investigated by Zhang *et al*. (2005, 2009). Comparing with ground-based measurements, satellite remote sensing has advantage about capturing the variation of dust storm in space and time, and was used to characterize the distribution of dust plumes in several studies (Husar *et al*., 2001; Darmenova *et al*., 2005; Huang *et al*., 2006). On the other hand, numerical modeling is an indispensable tool which was developed to predict the spatial and temporal of dust loading together with detailed physical and chemical properties (Gong *et al*., 2003; Liu *et al*., 2003; Shao *et al*., 2003), and many efforts have been

* Corresponding author.
E-mail address: mgzhang@mail.iap.ac.cn

made to enhance the reasonability of simulation (Shao, 2001; Shao *et al*., 2002; Park and In, 2003). For the direct radiative effect of dust, Wu *et al*. (2005) has used Regional Climate Model with a transport model and a radiative scheme of dust aerosol to simulate the direct radiative forcing of mineral dust over East Asia. The results show that the regional average values are quite variable and are obviously larger in spring than those in other seasons. Won *et al*. (2004) has investigated a dust event over Gosan, Korea and estimated its daily average direct radiative forcing. The analysis of that study shows the Asian dust has significant influence on radiation budget with quite large forcing values. At present, great achievements in Asian dust storm research are obtained with the progress of monitoring and modeling capability. However, the deficiencies in the understanding of the activities of dust and how it affects the regional environment and radiation balance still remain.

The strongest Asian dust storm in 2010 occurred from 19 to 21 March. As reported by National Meteorological Center of CMA (China Meteorological Administration), 16 provinces (cities) of China were hit by the dust storm, and the front of dust cloud could also reach the East China Sea and south sea areas of Japan on 21 March. The air pollution index (API) observed by Ministry of Environment Protection of China (MEP) exceeded 300 in several east cities in China, which means the dust caused heavy pollution in these cities. In this paper, we use air quality modeling system RAMS-CMAQ to simulate the distribution pattern and temporal evolution of this Asian dust event. The mass concentration, optical depth and direct radiative forcing of dust and other major aerosol species over East Asia are simulated and are validated with surface observations and satellite remote sensing data from MODIS in 18–21 March. The mechanism of dust particle emission generation and optical properties calculation module in the modeling system are improved for enhancing the accuracy of modeled results. Finally, we analyzed the modeled results for getting a throughout understanding about budget, optical properties, and the regional direct radiative effect of the dust storm. Since the dust storm generally happened in spring over East Asia while its direct radiative forcing reaches the highest, this typical case of the extreme dust event performance could give deeply recognize about how the dust particle influence the regional radiative balance.

MODEL DESCRIPTION

The modeling system has two major components: CMAQ and RAMS. CMAQ is a multi-scale and multi-pollutant air quality model, and could depict the detail processes about dust formation, transport, deposition, and other important characteristics (Byun and Ching, 1999). The comprehensive suite aerosol composition (sulfate, nitrate, ammonium, black carbon, organic mass, dust and sea salt) is taken into account. The aerosol particle size distribution is divided into three modes: Aitken mode, accumulation mode, and coarse mode. Table 1 lists the aerosol components, geometric standard deviation, and geometric mean radius of each mode. All modes were assumed to follow the lognormal distribution. Whereas internal mixing of the aerosol species is assumed within each mode, the modes themselves were externally mixed. The chemical mechanism CB05 (Sarwar *et al*., 2008) and aerosol evaluation processes of CMAQ Version 4.7 is used in this study, and the meteorological fields from RAMS instead of CMAQ default meteorological driver. RAMS is a highly versatile numerical code for simulating and forecasting meteorological phenomena, and has good ability to describe the boundary layer, which is important for simulating the dust formation. In this study, it is used to provide the three-dimension meteorological field for CMAQ, including boundary-layer turbulence, cloud, precipitation, and other meteorological elements. RAMS is exercised in a four-dimensional data assimilation mode using analysis nudging with reinitialization every 4 days, leaving the first 24 h as the initialization period. The background meteorological fields for RAMS were taken from the European Center for Medium-Range Weather Forecasts (ECMWF) analyzed datasets with 1° × 1° spatial resolution every six hours. Sea surface temperatures for RAMS were based on weekly mean values and observed monthly snow cover information. Some previous works have shown the reliability of the RAMS-CMAQ modeling system by comparing the simulation results with diverse measurement data (Zhang *et al*., 2003; Zhang *et al*., 2004a, b).

Dust emission plays an important role in dominating dust loading and deposition. In this study, we use an empirical mechanism (Han *et al*., 2004) to estimate the dust emissions. The mass flux could be approached by:

$$F = C \times u^4 \left(1 - \frac{u_*}{u}\right) \times (1 - fR), \quad u \geq u_* \tag{1}$$

where μ and μ_* are the friction and threshold friction velocities; C is a correction coefficient (1.4×10^{-15}) which controls the emission amount; R and f are the reduction factor and fractional coverage of vegetation in a model grid. For R, we choose 0.6 for grass, 0.7 for shrub and 0.1 for barren or sparsely vegetated land (Park and In, 2003). Fractional coverage, land use data, and other parameters used in formula (1) were well introduced in Han *et al*. (2004). This mechanism has good performance in several research works about dust numerical study. Han *et al*. (2004) also proved it to be reasonable for description Asian dust in modeling system. The emission inventories of other aerosol pollution (including gaseous precursors) from anthropogenic and natural sources for modeling system were well introduced by Han *et al*. (2010).

The aerosol optical depth (AOD) is simulated by a new parameterization which based on Mie theory, and could reasonably consider the refractive index, water uptake, and internal mixture factors while calculating aerosol optical properties. Comparison with satellite and ground-base *in situ* measurements showed that the modeled AOD is well consistent with observed results in previous work (Han *et al*., 2011). The vertical structure of dust flux is an important factor determining its long-range transport and intensity. Due to the lack of observation data of vertical mass distribution, the distribution of AOD can partly reflect the column content of aerosol mass concentrations. The direct radiative forcing

Table 1. Aerosol physical properties used in the modeling system.

Mode	Aerosol components	σ^a	$r_o{}^b$
Aitken	$ASO_4{}^c$, $ANO_3{}^d$, $ANH_4{}^e$, BC[f], OC[g]	1.7	0.015
Accumulation	ASO_4, ANO_3, ANH_4, BC, OC, Dust, Sea salt	2.0	0.150
Coarse dust	Dust	3.0	0.300
Coarse Sea salt	Sea salt	3.5	0.300

[a] geometric standard deviation.
[b] geometric mean radius.
[c] ASO_4 represents sulfate aerosol.
[d] ANO_3 represents nitrate aerosol.
[e] ANH_4 represents ammonium aerosol.
[f] BC represents black carbon.
[g] OC represents organic carbon.

is also estimated by radiative transfer scheme CAMRT (William *et al*., 2006) coupled with RAMS-CMAQ. For detail information (aerosol refractive index, hygroscopicity, density, ext.) about this simulation module of aerosol optical and radiative properties can be found in Han *et al*. (2011).

The model domain (Fig. 1) is 6645 × 5440 km^2 with a 64-km grid cell on a rotated polar stereographic map projection centered at (35°N, 116°E). The modeling system has 15 vertical layers in the coordinates system unequally spaced from the ground to ~23 km, with approximately half of them concentrated in the lowest 2 km to improve the simulation of the atmospheric boundary layer.

MODEL VALIDATION

Comparison with Surface Observations

The meteorology field is important to aerosol mass burden and direct forcing simulation. The accuracy of wind field and relative humidity simulation could obviously impact the dust particle transport and optical properties calculation. Thus, the measurement surface wind speed, wind direction, and relative humidity from the 325 m meteorological tower observation system at Beijing (Al-Jiboori *et al*., 2005) are used for validation. Fig. 2 shows the comparison results of hourly data during the dust storm period. It can be seen that the variation trend of modeled and observed wind speed and relative humidity coincide well with each other, especially for the diurnal variation. The modeled and observed wind directions do not agree very well. Except the deviation of model simulation, the main reason may be that the error of measurement from the influence of urban underlying surface around the meteorological tower. Additionally, since the

Fig. 1. Geographic location of API monitoring cities and CNMC measurement stations in the model domain.

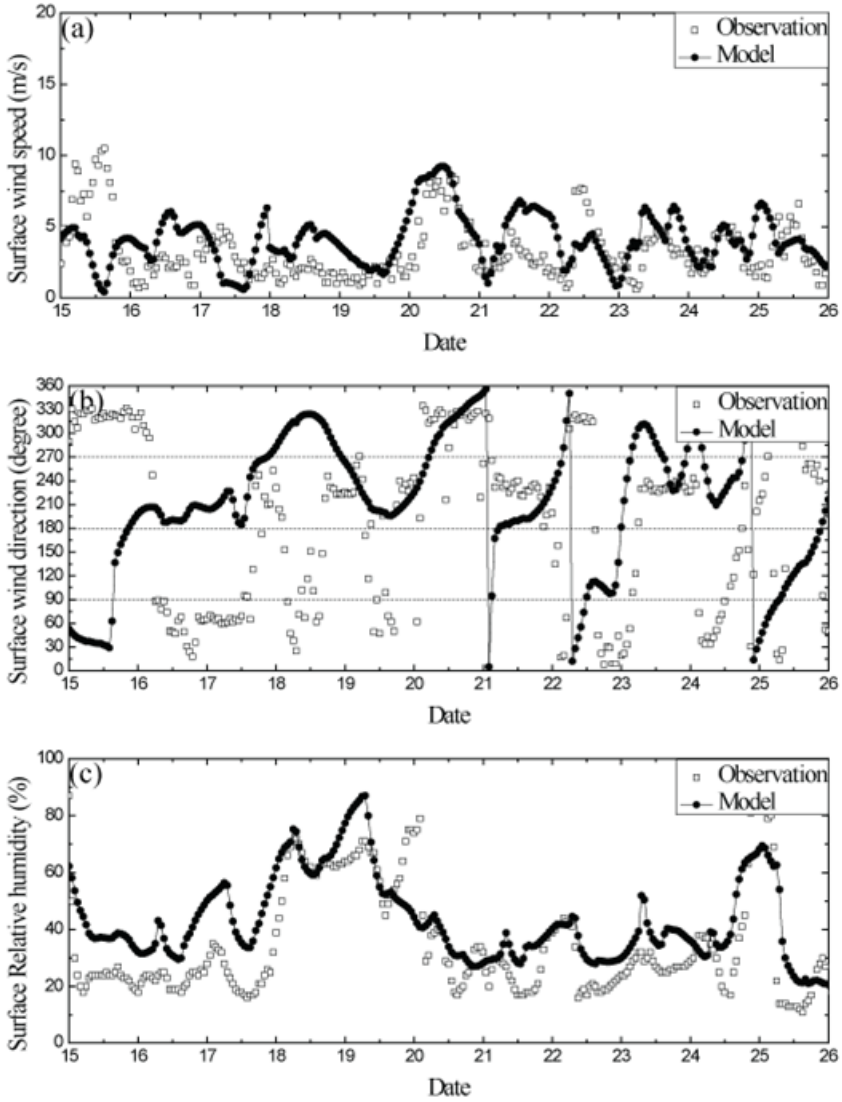

Fig. 2. The hourly surface wind speed (m/s) (a), wind direction (degree) (b), and relative humidity (%) (c) of model simulation and observation at Beijing from 15 to 25 March.

wind field is an important factor of the dust storm generation and transport simulation, the observed wind field data from surface stations of Chinese National Meteorological Centre (CNMC) (http://new-cdc.cma.gov.cn:8081/; Feng *et al*., 2004) are also collected in this paper for validation the modeled wind field. The observed data include the daily averaged wind speed and wind direction of daily maximum wind from 18 to 21 March at 19 stations which distributed throughout the regions influenced by dust event in China as shown in Fig. 1. The comparison results are shown in Fig. 3. It can be seen that the modeled wind speed could follow the values from observation relatively well. However, the observed wind speed become obviously higher at five mountain stations: Huangshan, Huashan, Nanyue, Taishan, and Wutaishan, but the modeled results could just capture the daily changing trend at these five stations and systematically lower than the observed results, which should be mainly caused by the disparity height between first layer of modeling system and measurement stations. The modeled daily maximum wind speed is generally lower than those of observations. The different time resolution of data obtaining between simulation (hourly) and measurement (ten minutes average) should be the main reasons of this underestimation. The main directions of modeled and observed wind directions are broadly same as shown in Figs. 3(c) and (d), which means the transport directions of aerosol particles will be generally correct during the dust storm period.

To evaluate the modeling system, we also collected the surface monitoring data of $PM_{2.5}$ and PM_{10} at two Beijing measurement sites, the API reported daily by MEP of China, and the satellite measurements over model domain for comparing with the modeling results. The observed $PM_{2.5}$ was collected by an intensive observation of an eight-stage cascade impactor (PIXE International Corp.) conducted at the top of an 8-m height building above the ground. The site was located in the Institute of Atmospheric Physics of Chinese Academy of Sciences (39°58'N, 116°22'E). The observed data of PM_{10} were provided by the measurements

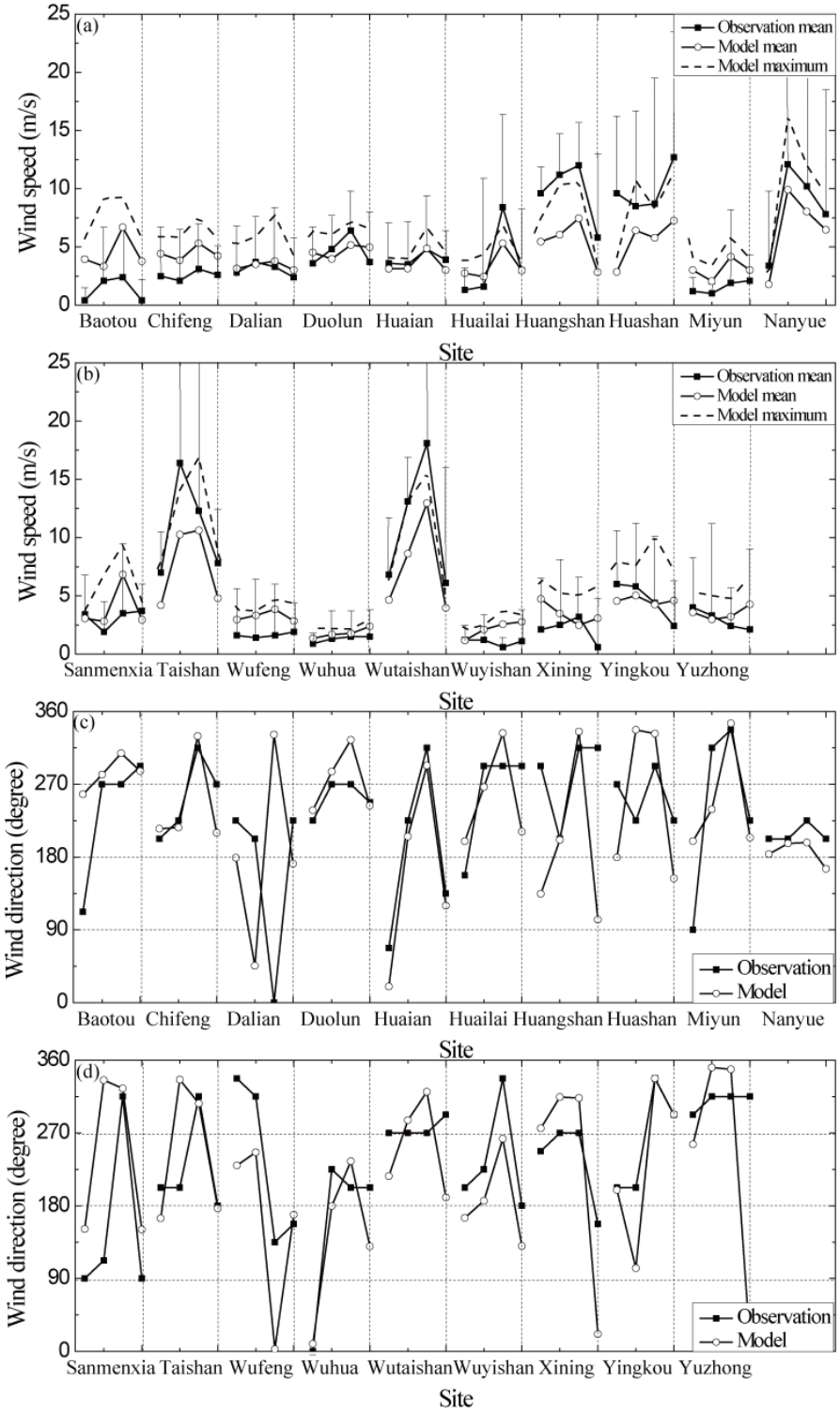

Fig. 3. The daily average wind speed, daily maximum wind speed (a–b), and wind direction of daily maximum wind (c–d) comparisons in 18–21 March at 19 surface stations of Chinese National Meteorological Centre. It includes four points that serially represented the values of measurement or simulation from 18 to 21 March at each station marked below the plots.

of an online particulate monitor of R & P TEOM 1400a which situated in the south suburban areas of Beijing (39°42′N, 116°21′E).

Fig. 4 shows the time series of observed and modeled 6-hour average mass concentration of $PM_{2.5}$ and PM_{10} at Beijing from 16 to 23 March, 2010. Generally, the model is broadly able to capture the observed data variation tendency, and both the simulated $PM_{2.5}$ and PM_{10} catch the two prominent peaks on 20 and 22 March at Beijing. The time and intensity of modeled and observed peak values show good

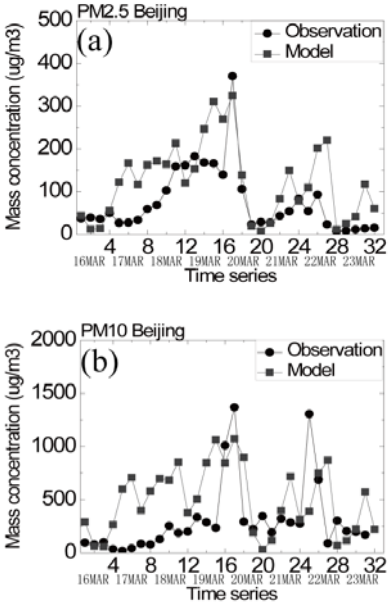

Fig. 4. Every 6-hourly average surface aerosol mass concentration (μg/m^3) of simulation and observation at Beijing from 16 to 23 March.

agreement in Figs. 4(a) and (b). The evident overestimate of modeled PM_{10} on 17 and 18 March is probably because the model results are interpreted as the average of each grid cell, and are influenced by the local pollution in Beijing.

API represents the air pollution level in Chinese cities (available at http://datacenter.mep.gov.cn) and is linearly related to the daily mean PM_{10} concentration of hourly observations. It can be described as following statement: when API (I) lies between the breakpoints I_i and I_j, the mass concentration of PM_{10} could be calculated by:

$$C = \frac{C_i - C_j}{I_i - I_j}\left(I - I_j\right) + C_j \quad (2)$$

where C is the PM_{10} concentration, C_i and C_j are the PM_{10} concentrations corresponding to I_i and I_j which are listed in Table 2. It should be noted that the upper limitation of API is 500, which means the PM_{10} daily averaged concentration larger than 600 μg/m^3 would not be reported.

In this paper, the API data of twelve cities which locate near the dust source regions or on dust storm transport pathway in China is selected and converted into mass concentrations for validating the modeled surface PM_{10} from 10 to 30 March. Fig. 5 shows the positions of selected cities in model domain and comparison results, respectively. The site locations and statistical parameters of comparisons are listed in Table 3. The correlation coefficients (R) in Table 3 are all significant at the 0.05 level. In Fig. 3 it can be seen that the cities Huhhot and Datong are located near the dust source region. The observed PM_{10} concentrations at these two cities shown in Fig. 5 both reached the maximum 600 μg/m^3 on 20 March when the dust storm occurred. The model results could reproduce this feature well and the highest value could reach more than 800 μg/m^3. The R between simulations and observations given in Table 3 are 0.85 and 0.74 at these two cities, respectively, which means the modeling system performs well near the dust source region. At Beijing, Jinan, Lanzhou, and Xi'an, four cities in the north part of China, the modeling system could also broadly capture the high values of PM_{10} concentrations appeared from 20 to 22 March. The R is higher than 0.50 at Beijing, Jinan, and Xi'an. However, the model underestimated PM_{10} concentrations in 13–15 March at Lanzhou which might be caused by the complex terrain and underlying surface conditions, so that the R does not reach 0.50. The maximum of simulation PM_{10} concentrations at three southern cities of China, Nanchang, Hangzhou, and Shanghai, appeared on 21 March. It is one day later than those of northern cities of China and corresponds well with the measurement results. Additionally, it can be found that the PM_{10} concentrations became relatively lower during the dust storm period at the rest three cities, Changsha, Fuzhou, and Guangdong, which are located in the Southeast China, and the modeling system could also basically reflect this phenomenon. The R could exceed 0.5 at these six southern cities of China except Guangzhou. The lower correlation coefficient at Guangzhou might be caused by the overestimate of modeled PM_{10} concentrations from 17 to 21 March.

Table 2. The breakpoints of API and corresponding PM_{10} concentrations.

API	0	50	100	200	300	400	500
PM_{10} (μg/m^3)	0	50	150	350	420	500	600

Comparison with Satellite Retrievals

Fig. 6 shows the MODIS images during the dust events over China and the distribution plots of surface dust concentration simulated by modeling system. In the MODIS images, yellow regions represent the dust plume, and the deep yellow indicates heavier dust burden. The white regions represent the rejected observational data over bright land surface due to the high retrieval uncertainty for MODIS. Even though the quantity of dust mass burden is not detected, the concentrating regions and transport pathway of dust storm is shown clearly in the MODIS images. It can been seen that the observed and simulated dust distribution features generally agree with each other during the dust event, especially on 20 March when the heaviest dust storm appeared in the Mid-Eastern China. It demonstrates that the modeling system has good abilities to reproduce the spatial and temporal patterns of dust aerosol.

Fig. 7 shows the daily averaged AOD distributions derived from modeling system simulation and MODIS instruments retrieval during the dust event. The modeled daily mean of AOD in Fig. 7 only used data from 10AM and 2PM (local time) encompassing MODIS satellite overpass times. The highest AOD values in the model domain ranged from 1.5 to 2.0, which are significantly larger than the global mean value 0.15 estimated by satellite measurements (Kinne *et al*., 2006). It can be said that dust aerosol was one of the major contribution species in the high AOD regions because those regions are coincided with the high dust burdens shown

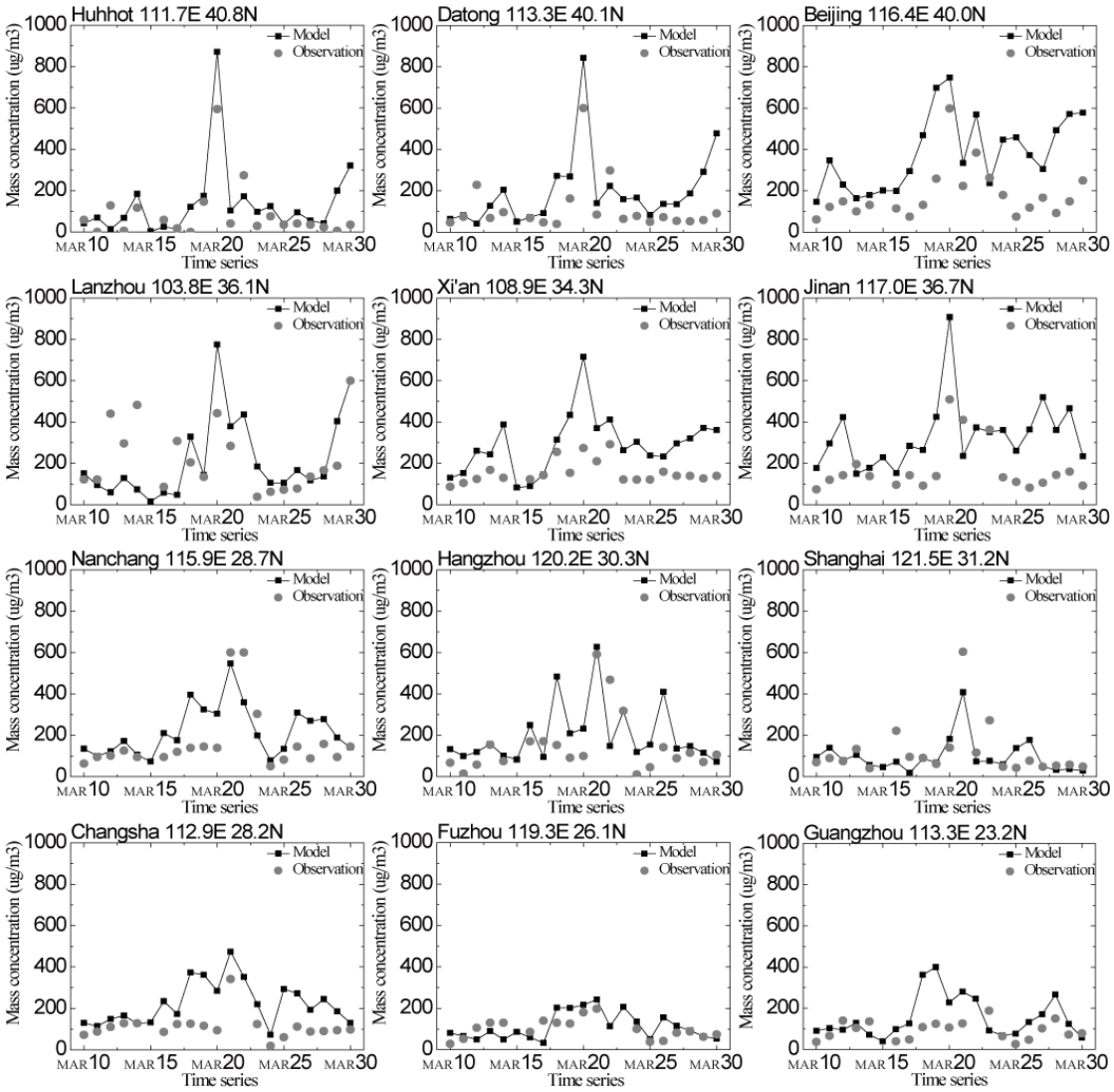

Fig. 5. Comparisons of the modeled and the observed daily averaged PM_{10} concentrations (μg/m^3) in 12 cities of China.

Table 3. Statistical summary of the comparisons of daily averaged PM_{10} between observations and simulations in 12 cities.

	Site	Location	N^a	$C_{obs}{}^b$	$C_{mod}{}^c$	$\sigma_{obs}{}^d$	$\sigma_{mod}{}^e$	R^f
1	Huhhot	111.7°E, 40.8°N	18	95.53	146.84	136.70	192.39	0.85
2	Datong	113.3°E, 40.1°N	20	116.35	203.07	128.06	177.25	0.74
3	Beijing	116.4°E, 40.0°N	20	181.16	391.93	123.50	174.76	0.63
4	Lanzhou	103.8°E, 36.1°N	19	224.25	213.66	159.66	193.03	0.49
5	Xi'an	108.9°E, 34.3°N	20	156.57	302.23	55.23	113.75	0.65
6	Jinan	117.0°E, 36.7°N	19	170.87	337.59	117.27	169.96	0.53
7	Fuzhou	119.3°E, 26.1°N	18	99.56	108.78	46.24	65.20	0.55
8	Hangzhou	120.2°E, 30.3°N	20	150.57	206.57	143.78	142.92	0.62
9	Shanghai	121.5°E, 31.2°N	20	119.31	99.39	125.59	83.82	0.79
10	Changsha	112.9°E, 28.2°N	19	110.47	221.03	60.69	100.41	0.65
11	Nanchang	115.9°E, 28.7°N	20	169.20	227.66	152.21	116.51	0.70
12	Guangzhou	113.3°E, 23.2°N	19	92.63	156.38	43.53	99.25	0.36

[a] Number of samples.
[b] Total mean of observations (μg/m^3).
[c] Total mean of simulations (μg/m^3).
[d] Standard deviation of observations.
[e] Standard deviation of simulations.
[f] Correlation coefficient between daily observation and simulation.

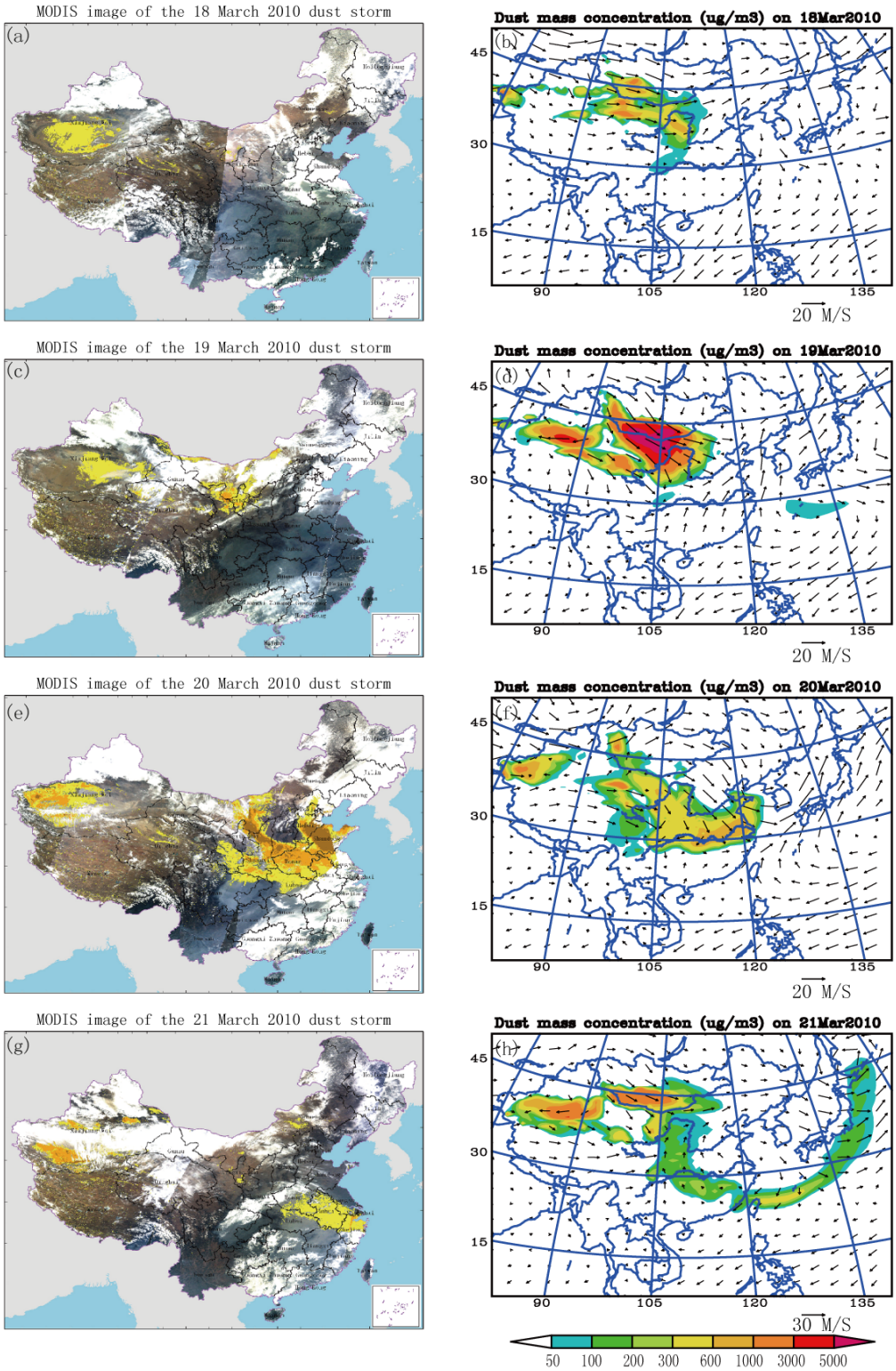

Fig. 6. MODIS images of dust storm (left) over China and modeled surface dust concentration (μg/m^3) (right) in 18–21 March.

in Fig. 7 (see more analysis in the next section). The comparison in Fig. 6 presents that the distribution patterns over Southeast China and sea areas of simulated AOD are generally similar to the satellite measurement results over Eastern China and sea areas during the dust events, which indicates the modeling system can reasonably well predict the optical depth of dust and other aerosol species over these regions. However, the simulated AOD values are probably lower than the MODIS AOD over Western China (The model results are hard to be validated over this region because of the rare measurement data). The reasons might be that the aerosol burden here is relatively underestimated by modeling

system, and some deviation might be existent on the AOD products of MODIS instruments over inland area in East Asia as well (Xia *et al*., 2005). Hsu *et al*. (2006) also pointed out that the dark-target approach of MODIS inverse method performs not well enough over the arid and semiarid areas with bare soil land, such as the physiognomy in Northwest China.

From the evaluations discussed above, it can be concluded that the modeling system is able to reproduce the distribution and transport features of aerosol burden and optical depth reasonably well, which supports the model analyses of dust storm evolution could be reliable.

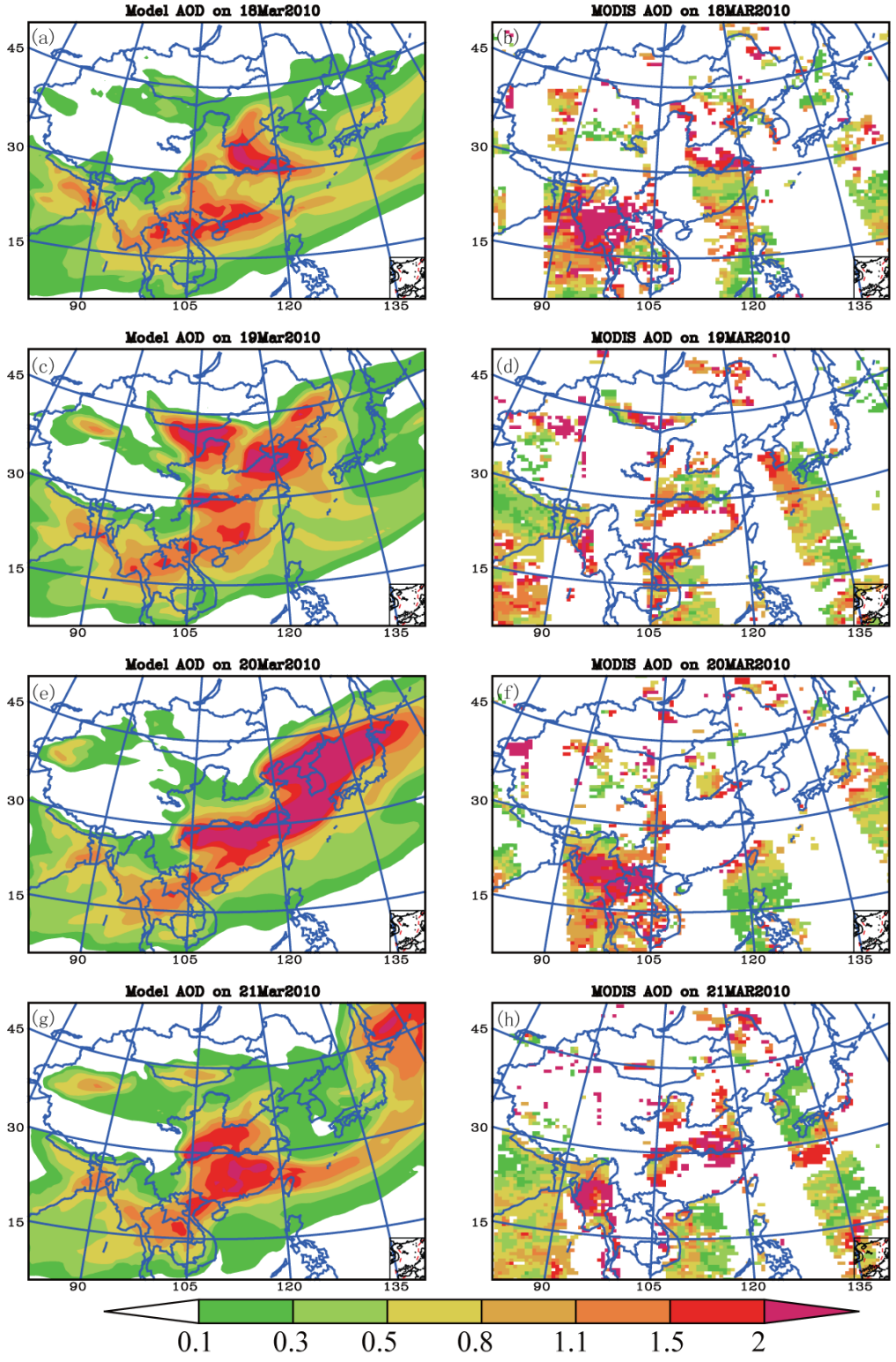

Fig. 7. Aerosol optical depth at 550 nm in 18–21 March from model simulations (left) and from satellite measurements (right).

MODEL RESULTS

Dust Formation, Transport, and Spatial Distribution

The spatio-temporal continuity of simulation data could help us improve the understanding of the detail information about physical and optical characteristics of dust storm in March 2010. From the simulation results, the dust storm could be described as follow: the surface dust burden on 18 March in Fig. 7(b) shows that the strong northwesterly winds (10–20 m/s) over Gobi desert caused by cold air flow associated with a Mongolian Cyclone generated up to 500 μg/m^3 dust aerosol over the south of Mongolia and Northwest China. On 19 March, the northwesterly winds over most parts of Gobi desert exceeded 20 m/s, while the surface dust concentration exceeded 1000 μg/m^3 (Fig. 7(d)). The extremely highest dust concentration which reached 5000 μg/m^3 in southern Mongolia and western Inner Mongolia province of China was far more than those of other aerosol species. Fig. 7(f) shows the dust cloud followed the northwesterly wind prevail and transported from north part to central and east part of China on 20 March. We can see in most parts of North China, Central China, and East China the strong wind field with high wind speed ranging from 15 to 20 m/s appeared. The surface dust concentration was about 300–600 μg/m^3 in the stripes zone between Yellow River and Yangtze River, and in the lower-middle reaches of the Yangtze River the maximum went up to 600 μg/m^3. The populated eastern seaboard of China was seriously affected by the dust storm weather on 20 March. Fig. 7(h) shows that the first dust cloud arrived in the Southeast China, East China Sea and Western Pacific to the south of Japan on 21 March. It can be found the dust concentration ranged from 100 μg/m^3 to 300 μg/m^3 over Southeast China, and exceeded 300 μg/m^3 over the East China Sea.

Dust Column Burden, Contribution to AOD, and Direct Radiative Forcing

Fig. 8 presents the daily averaged column burden of dust in 18–21 March from model simulations. It can be said that the obviously heavy dust burden appeared over Central China on 18 March shown in Fig. 8(a) was the dust plume that convected to higher layer of atmosphere since it did not appear in Fig. 7(b). The similar situation also happened over North China and Central China on 20 and 21 March, respectively. The highest dust column burden could exceed 3000 mg/m^2 over dust source region on 19 March and North China on 20 March.

Fig. 9 presents the daily averaged AOD and dust contribution which is shown as percentage of total AOD. The dust contribution is obtained by subtracting AOD with and without dust. It can be found that the regions of contribution exceeded 20% mainly appeared over those AOD larger than 0.1 during these four days, which means dust aerosol was one of the major contribution species over model domain. The regions with more than 50% dust concentration were mainly near the dust source region in Northwest China and Mongolia, where AOD ranged from 0.1 to 0.8 on 18, 19, and 21 March. The high value regions of AOD ranging from 1.1 to 2.0 over western Inner Mongolia province of China had more than 80% contribution from dust on 19 March. The regions with 50% dust contribution extended to Central China and part of North China when the heaviest dust storm appeared over these regions and the highest AOD was around 2.0 on 20 March. It indicated that the dust particles could strongly influence the local radiative effects over these areas. Analyzing the mass concentrations of dust shown in Fig. 8, it can be concluded that the AOD mainly contributed by dust could exceed 0.5 and 1.5 when the column burden of dust reaches 1000 mg/m^2 and 3000 mg/m^2, respectively.

The daily direct radiative forcing of dust at top-of-atmosphere (TOA) which is obtained by subtracting the radiative effects with all aerosol species and without dust in all-sky case during the dust storm period is shown in Fig. 10. It can be found that the distribution patterns of dust radiative forcing were generally following its column burden patterns. The strong radiative forcing mainly concentrated over the regions where heavy dust burden and high contribution to AOD from dust located. The low values of dust radiative forcing were mainly ranged from –10 to –2 W/m^2 on 18 and 21 March over Central China and sea areas while the dust column burden ranging from 300 to 1000 mg/m^2. When dust column burden exceeded 1000 mg/m^2, it can be seen that the radiative forcing could reach –25 to –10 W/m^2 over North China and the stripes zone between Yellow River and Yangtze River of China on 19 and 20 March, respectively. This value range is similar with the strongest direct radiative forcing of all major aerosol species over East Asia given by some relative work (Qian et al., 2003; Won et al., 2004; Liu *et al*., 2007). The strongest dust radiative forcing appeared on 19 March when its column burden exceeded 3000 mg/m^2 over western Inner Mongolia province of China. The lowest value could reach –30 W/m^2 and provided very strong negative radiative effect over this area. This phenomenon indicated that the Asia dust plume could obviously influence the radiative balance for the large forcing values of one dust event and the dust events occur frequently in the East Asia in spring (Murayama *et al*., 2001; Sun *et al*., 2001)

DISCUSSION AND CONCLUSIONS

The dust storm occurred in 18–21 March was the strongest Asian dust event in 2010. We implemented RAMS-CMAQ to simulate the mass concentration, optical depth, and direct radiative forcing at TOA of dust and other major aerosol components, including sulfate, nitrate, ammonium, black carbon, organic carbon, and sea salt, during the dust event. The estimation of dust emission is based on a mechanism considering specific land-surface conditions and meteorological fields over model domain. The aerosol optical and radiative properties were calculated by a parameterization which could reflect multiple aerosol microphysical properties and a radiative transfer scheme CAMRT. The modeling system performance is fully evaluated by comparing with mass concentration and API from surface observations and satellite measurements from MODIS instrument. The comparison results show that the modeling system performs well on simulating dust mass concentration and AOD distributions.

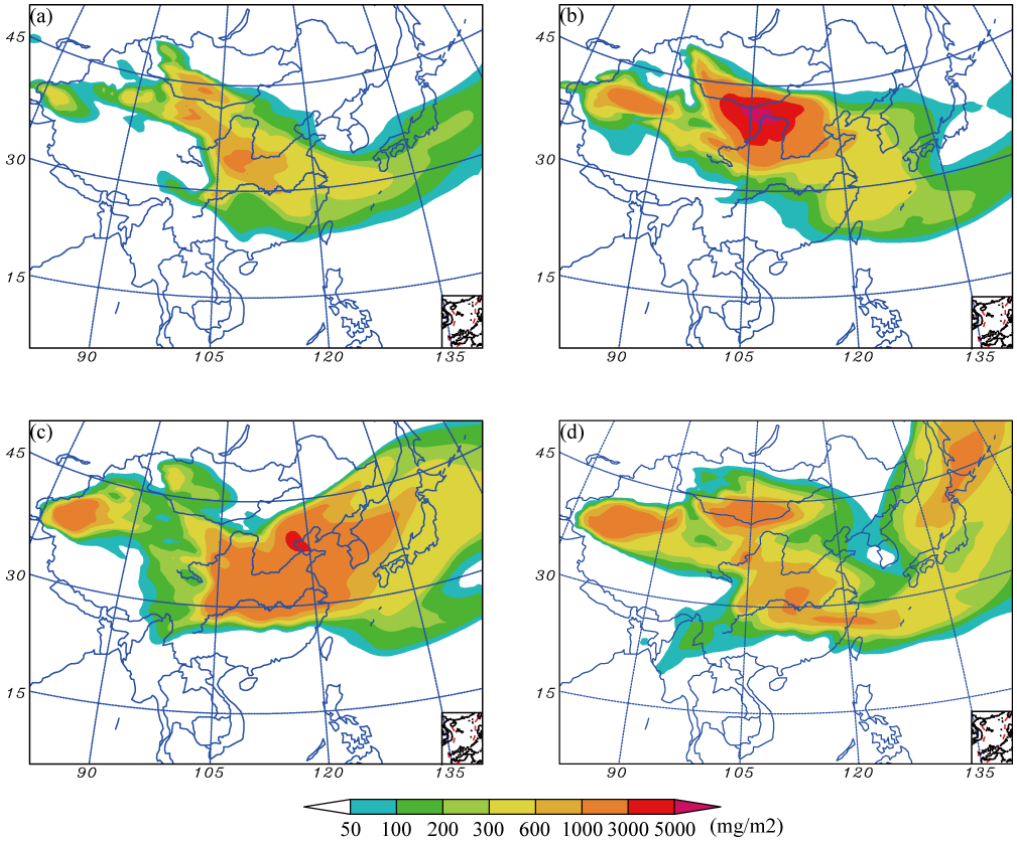

Fig. 8. Daily averaged column burden (mg/m^2) of dust on 18(a), 19(b), 20(c), and 21(d) March.

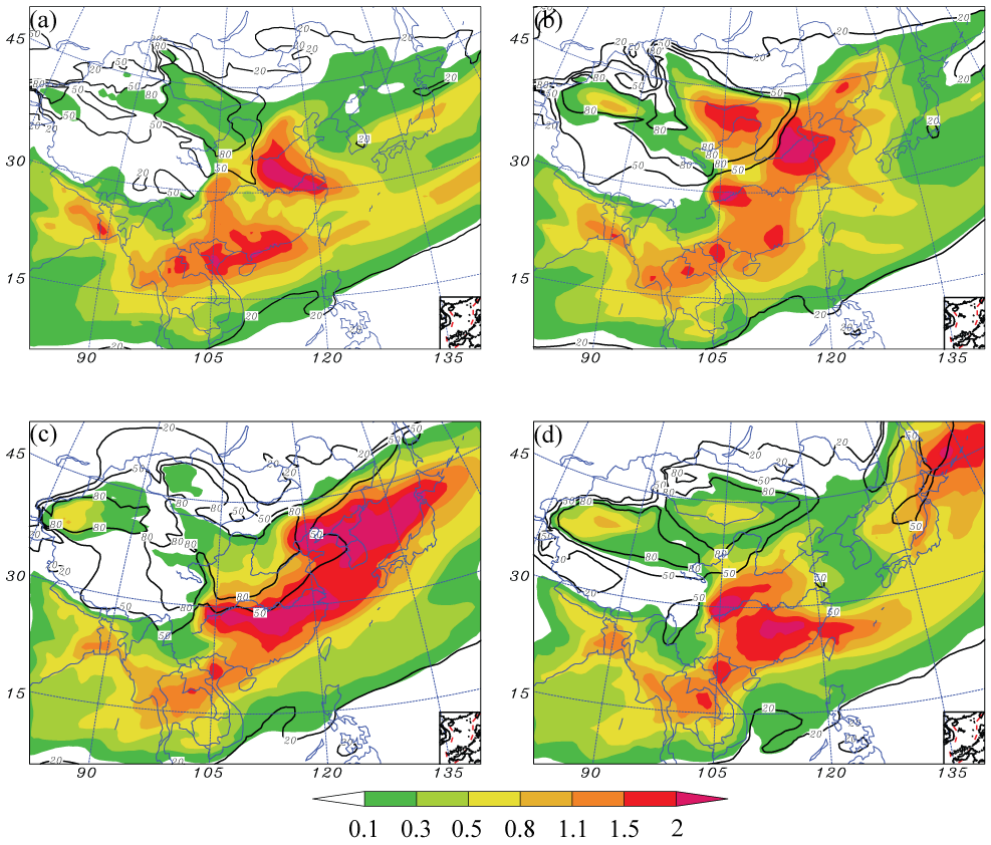

Fig. 9. Daily averaged AOD on 18(a), 19(b), 20(c), and 21(d) March. Contour lines show the contribution of dust (%).

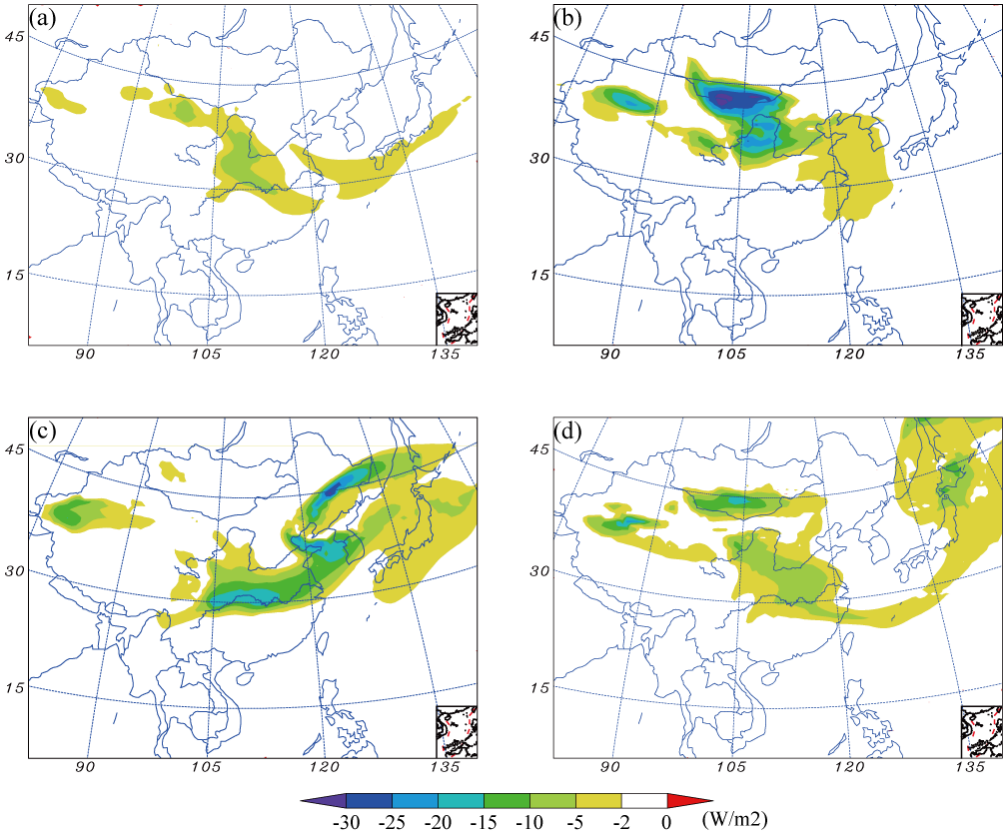

Fig. 10. Daily averaged direct radiative forcing of dust at top-of-atmosphere on 18(a), 19(b), 20(c), and 21(d) March (W/m^2).

From simulation results, it is easy to find out the features of dust cloud transport routine and the wind field variation during the whole period of the dust event. It is shown clearly that the dust storm broke out on 19 March, and formed over the dust source regions: Taklamakan Deserts and Gobi Desert, and then swept central and eastern China. The dust storm also strongly influenced south part of China, such as Pearl River Delta region, and East China Sea area. The daily high values of surface dust concentrations could exceed 3000 μg/m^3 over the source regions and decreased to about 100 μg/m^3 over the downward regions. Although the values decreased sharp, the surface dust concentrations were still obviously higher than the normal level over the downstream zones. It can be seen that the surface dust concentration still exceeded 300 μg/m^3 over East China Sea area on 21 March. As the reports of Central Meteorological Observatory of China, the values over some places (e.g., Taiwan province) got a new record of the worst sandstorm conditions ever since during this dust event period.

From model simulation it can also be found that the high values of AOD mainly contributed by dust appeared over Gobi desert on 19 March, lower-middle reaches of the Yangtze River on 20 March and East China Sea on 21 March. The heavy dust storm generated very strong extinction effects, and would obviously alter the regional visibility and radiation balance over these regions. The direct radiative forcing of dust verified this phenomenon with the lowest value around –30 W/m^2 appeared over western Inner Mongolia province of China on 19 March. The high column burden of dust which exceeds 1000 mg/m^2 could cause more than –10 W/m^2 radiative forcing over the regions dust storm swept. This value is about equal to the strongest radiative forcing of total aerosol species in normal period without dust storm over East Asia.

In this paper, the modeling system RAMS-CMAQ has been fully evaluated on dust burden and optical depth simulations and gives clear understanding about the mass burden and radiative effect of dust storm. In future work, it can be applied to forecast and analyze the dust events over East Asia as one kind of effective tool.

ACKNOWLEDGEMENT

This work was supported by National Department Public Benefit Research Foundation (Ministry of Environmental Protection of the People's Republic of China) (No. 201009001, 201109002).

REFERENCE

Al-Jiboori, M.H. and Hu, F. (2005). Surface Roughness around a 325-m Meteorological Tower and its Effect on Urban Turbulence. *Adv. Atmos. Sci.* 22: 595–605.

Byun, D.W. and Ching, J. (1999). Science Algorithms of the EPA Models-3 Community Multi-scale Air Quality (CMAQ) Modeling System, NERL, Research Triangle Park, NC, pp. 425.

Chen, Y., Sheen, P., Chen, E., Liu, Y., Wu, T. and Yang, C.

(2004). Effects of Asian Dust Storm Events on Daily Mortality in Taipei, Taiwan. *Atmos. Environ.* 95: 151–155.

Chun, Y., Boo, K.O., Kim, J., Park, S.U. and Lee, M. (2002). Synopsis, Transport, and Physical Characteristics of Asian Dust in Korea. *J. Geophys. Res.* 106: 18461–18469.

Darmenova, K., Sokolik, I.N. and Darmeov, A. (2005). Characterization of East Asian Dust Outbreaks in the Spring of 2001 Using Ground-based and Satellite Data. *J. Geophys. Res.* 110: D02204, doi: 10.1029/2004JD004842.

Feng, S., Hu, Q. and Qian, W. (2004). Quality Control of Daily Meteorological Data in China, 1951-2000: A New Dataset. *Int. J. Climatol.* 24: 853–870.

Ghan, S. and Rahul, A.Z. (2007). Parameterization of Optical Properties for Hydrated Internally Mixed Aerosol. *J. Geophys. Res.* 112: D10201, doi: 10.1029/2006JD007927.

Gong, S.L., Zhang, X.Y., Zhao, T.L., McKendry, I.G., Jaffe, D.A. and Lu, N.M. (2003). Characterization of Soil Dust Aerosol in China and its Transport and Distribution during 2001 ACE-Asia: 2. Model Simulation and Validation. *J. Geophys. Res.* 108: 4262, doi: 10.1029/2002JD002633.

Han, X., Zhang, M.G., Han, Z.W., Xin, J.Y., Wang, L.L., Qiu, J.H. and Liu, Y.J. (2010). Model Analysis of Aerosol Optical Depth Distributions over East Asia. *Sci. China Earth Sci.* 53: 1–12.

Han, X., Zhang, M.G., Han, Z.W., Xin, J.Y. and Liu, X. (2011). Simulation of Aerosol Direct Radiative Forcing with RAMS-CMAQ in East Asia. *Atmos. Environ.* 45: 6576–6592

Han, Z., Ueda, H., Matsuda, K., Zhang, R., Arao, K., Kanai, Y., Hasome, H. (2004). Model Study on Particle Size Segregation and Deposition during Asian Dust Events in March 2002. *J. Geophys. Res.* 109: D19205, doi: 10.1029/2004JD004920.

Hsu, N., Tsay, S., King, M. and Herman, J. (2006). Deep Blue Retrievals of Asian Aerosol Properties during ACE-Asia. *IEEE Trans. Geosci. Remote Sens.* 44: 3180–3199

Huang, J.P., Minnis, P., Lin, B., Wang, T.H., Yi, Y.H., Hu, Y.X., Sun-Mack, S. and Ayers, K. (2006). Possible Influences of Asian Dust Aerosols on Cloud Properties and Radiative Forcing Observed from MODIS and CERES. *Geophys. Res. Lett.* 33: L06824, doi: 10.1029/2005GL024724.

Husar, R.B., Tratt, D.M., Schichtel, B.A., Falke, S.R., Li, F., Jaffe, D., Gassó, S., Gill, T., Laulainen, N.S., Lu, F., Reheis, M.C., Chun, Y., Westphal, D., Holben, B.N., Gueymard, C., McKendry, I., Kuring, N., Feldman, G.C., McClain, C., Frouin, R.J., Merrill, J., DuBois, D., Vignola, F., Murayama, T., Nickovic, S., Wilson, W.E., Sassen, K., Sugimoto, N. and Malm, W.C. (2001). Asian Dust Events of April 1998. *J. Geophys. Res.* 106: 18317–18330.

Intergovernmental Panel on Climate Change (IPCC) (2007). Changes in Atmospheric Constituents and in Radiative Forcing, In *Climate Change 2007*, Cambridge Univ. Press, New York.

Kinne, S., Schulz, M., Textor, C., Guibert, S., Balkanski, Y., Bauer, S.E., Berntsen, T., Berglen, T.F., Boucher, O., Chin, M., Collins, W., Dentener, F., Diehl, T., Easter, R., Feichter, J., Fillmore, D., Ghan, S., Ginoux, P., Gong, S., Grini, A., Hendricks, J., Herzog, M., Horowitz, L., Isaksen, I., Iversen, T., Kirkevåg, A., Kloster, S., Koch, D., Kristjansson, J.E., Krol, M., Lauer, A., Lamarque, J.F., Lesins, G., Liu, X., Lohmann, U., Montanaro, V., Myhre, G., Penner, J., Pitari, G., Reddy, S., Seland, O., Stier, P., Takemura, T. and Tie, X. (2006). An AeroCom Initial Assessment Optical Properties in Aerosol Component Modules of Global Models. *Atmos. Chem. Phys.* 6: 1815–1834.

Kurosaki, Y. and Mikami, M. (2003). Recent Frequent Dust Events and their Relation to Surface Wind in East Asia. *Geophys. Res. Lett.* 30: 1736, doi: 10.1029/2003GL017261.

Liu, M., Westphal, D.L., Wang, S.G., Shimizu, A., Sugimoto, N., Zhou, J., and Chen, Y. (2003). A High-resolution Numerical Study of the Asian Dust Storms of April 2001. *J. Geophys. Res.* 108: 8653, doi: 10.1029/2002JD003178.

Liu, X., Pernner, J.E., Das, B., Bergmann, D., Rodriguez, J.M., Strahan, S., Wang, M.H. and Feng, Y. (2007). Uncertainty in Global Aerosol Simulation: Assessment Using Three Meteorological Data Sets. *J. Geophys. Res.*, 112, D11212, doi: 10.1029/2006JD008216.

Murayama, T., Sugimoto, N., Uno, I., Kinoshita, K., Aoki, K., Hagiwara, N., Liu, Z.Y., Matsui, I., Sakai, T., Shibata, T., Arao, K., Sohn, B.J., Won, J.G., Yoon, S.C., Li, T., Zhou, J., Hu, H.L., Abo M., Iokibe, K., Koga, R. and Iwasaka, Y. (2001). Ground-based Network Observation of Asian Dust Events of April 1998 in East Asia. *J. Geophys. Res.* 106: 18345–18359.

Park, S.U. and In, H.J. (2003). Parameterization of Dust Emission for the Simulation of the Yellow Sand (Asian Dust) Event Observed in March 2002 in Korea. *J. Geophys. Res.* 108: 4618, doi: 10.1029/2003JD003484.

Qian, W.H., Quan, L.S. and Shi, S.Y. (2002). Variations of the Dust Storm in China and its Climatic Control. *J. Climate* 15: 1216–1229.

Qian, Y., Leung, L.R., Ghan, S.J. and Giorgi, F. (2003). Regional Climate Effects of Aerosols over China: Modeling and Observation. *Tellus Ser. B* 55: 914–934.

Sarwar, G., Luecken, D., Yarwood, G., Whitten, G. and Carter, W. (2008). Impact of an Updated Carbon Bond Mechanism on Predictions from the CMAQ Modeling System: Preliminary Assessment. *J. Appl. Meteor. Climatol.* 47: 3–14.

Sassen, K. (2002). Indirect Climate Forcing over the Western US from Asian Dust Storms. *Geophys. Res. Lett.* 29: 1465, doi: 10.1029/2001GL014051.

Satheesh, S.K. and Ramanathan, V. (2000). Large Differences in the Tropical Aerosol Forcing at the Top of the Atmosphere and Earth's Surface. *Nature* 405: 60–63.

Shao, Y. (2001). A Model for Mineral Dust Emission. *J. Geophys. Res.* 106: 20239–20254.

Shao, Y., Jung, E.J. and Leslie, L.M. (2002). Numerical Prediction of Northeast Asian Dust Storms Using an Integrated Wind Erosion Modeling System. *J. Geophys. Res.* 107: 4814–4836.

Shao, Y., Yang, Y., Wang, J.J., Song, Z.X., Leslie, L.M., Dong, C.H., Zhang, Z.H., Lin, Z.H., Kanai, Y., Yabuki, S. and Chun, Y.S. (2003). Northeast Asian Dust Storms: Real-time Numerical Prediction and Validation. *J. Geophys. Res.* 108: 4691, doi: 10.1029/2003JD003667.

Sun, J., Zhang, M. and Liu, T. (2001). Spatial and Temporal Distribution of Dust Storms in China and its Surrounding Regions, 1960–1999: Relations to Source Area and Climate. *J. Geophys. Res.* 106: D10, 10325–10333.

Tratt, D.M., Frouin, R.J., Westphal, D.L. (2001). April 1998 Asian Dust Event: A Southern California Perspective. *J. Geophys. Res.* 106: 18371–18379.

Wang, J., Xia, X.A., Wang, P.C. and Christopher, S.A. (2004). Diurnal Variability of Dust Aerosol Optical Thickness and Angstrom Exponent over Dust Source Regions in China. *Geophys. Res. Lett.* 31: L08107, doi: 10.1029/2004GL019580.

William, D.C., Rasch, P.J., Boville, B.A., Hack, J.J., McCaa, J.R., Williamson, D.L., Briegleb, B.P., Bitz, C.M., Lin, S.J. and Zhang, M.H. (2006). The Formulation and Atmospheric Simulation of the Community Atmosphere Model Version 3 (CAM3). *J. Climate* 19: 2144–2161.

Won, J., Yoon, S., Kim, S., Jefferson, A., Dutton, E.G. and Holben, B.N. (2004). Estimation of Direct Radiative Forcing of Asian Dust Aerosols with Sun/Sky Radiometer and Lidar Measurement at Gosan, Korea. *J. Meteor. Soc. Japan* 82: 115–130.

Wu, J., Fu, C., Jiang, W., Liu, H. and Zhao, R. (2005). A Preliminary Simulation Study of Direct Radiative Forcing of Mineral Dust Aerosol over the East Asia Region. *Chinese J. Geophys.* 48: 1250–1260. (In Chinese)

Xia, X.A., Chen, H.B. and Wang, P.C. (2005). Validation of MODIS Aerosol Retrievals and Evaluation of Potential Cloud Contamination in East Asia. *J. Environ. Sci.* 16: 832–837.

Zhang, M.G., Uno, I., Carmichael, G.R., Akimoto, H., Wang, Z., Tang, Y. Woo, J.H., Streets, D.G., Sachse, W.G., Avery, M.A., Weber, R.J. and Talbot, R.W. (2003). Large-scale Structure of Trace Gas and Aerosol Distributions over the Western Pacific Ocean during TRACE-P. *J. Geophys. Res.* 108, doi: 10.1029/2002JD002946.

Zhang, M.G., Uno, I., Yoshida, Y., Xu, Y., Wang, Z., Akimoto, H., Bates, T., Quinn, T., Bandy, A. and Blomquist, B. (2004a). Transport and Transformation of Sulfur Compounds over East Asia during the TRACE-P and ACE-Asia Campaigns. *Atmos. Environ.* 38: 6947–6959.

Zhang, M.G. (2004b). Modeling of Organic Carbon Aerosol Distributions over East Asia in the Springtime. *China Part.* 2: 192–195.

Zhang, R.J., Arimoto, R., An, J.L., Yabuki, S. and Sun, J.H. (2005). Ground Observations of a Strong Dust Storm in Beijing in March 2002. *J. Geophys. Res.* 110: D18S06, doi: 10.1029/2004JD004589.

Zhang, R.J., Han, Z.W., Cheng, T.T. and Tao, J. (2009). Chemical Properties and Origin of Dust Aerosols in Beijing during Springtime. *Particuology* 7: 61–67.

Zhang, X.Y., Gong, S.L., Shen, Z.X., Mei, F.M., Xi, X.X., Liu, L.C., Zhou, Z.J., Wang, D., Wang, Y.Q. and Cheng, Y. (2003a). Characterization of Soil Dust Aerosol in China and its Transport and Distribution during 2001 ACE-Asia: 1. Network Observations. *J. Geophys. Res.*, 108: 4261, doi: 10.1029/2002JD002632.

Zhang, X.Y., Gong, S.L., Zhao, T.L., Arimoto, R., Wang, Y.Q. and Zhou, Z.J. (2003b). Sources of Asian Dust and Role of Climate Change versus Desertification in Asian Dust Emission. *Geophys. Res. Lett.* 30: 2272, doi: 10.1029/2003GL018206.

Received for review, November 7, 2011
Accepted, May 11, 2012